Technical report

Flexural Behaviour of Reinforced Lightweight Concrete Beams Made with Oil Palm Shell (OPS)

Delsye C. L. Teo[1], Md. Abdul Mannan[2] and John V. Kurian[3]

Received 3 May 2006, accepted 11 August 2006

Abstract

This paper presents an investigation on the flexural behaviour of reinforced concrete beams produced from oil palm shell (OPS) aggregates. Utilising OPS in concrete production not only solves the problem of disposing this solid waste but also helps conserve natural resources. A total of 6 under-reinforced beams with varying reinforcement ratios (0.52% to 3.90%) were fabricated and tested. Data presented include the deflection characteristics, cracking behaviour, ductility indices and end-rotations. The investigation revealed that the flexural behaviour of reinforced OPS concrete beams was comparable to that of other lightweight concretes and the experimental results compare reasonably well with the current Codes of Practice. It was observed that beams with low reinforcement ratios satisfied all the serviceability requirements as per BS 8110.

1. Introduction

Malaysia is currently producing more than half of the world's total output of palm oil, planted over 4.05 million hectares of land, yielding about 18.88 tonnes/hectare of fresh fruit bunch (FFB) (MPOB 2006). At the mills where the FFB are processed and oil extraction takes place, solid residues and liquid wastes are generated. These wastes include empty fruit bunches, fibre, shell and effluent. In general, the fresh fruit bunches (FFB) contains about 5.5 % shell (Ma *et al*., 1999) and consequently, over 4 million tonnes of oil palm shell (OPS) solid waste is produced annually. This waste is normally disposed through incineration and at times, the shell is left to rot in huge mounds as shown in **Fig. 1**. This will ultimately cause pollution and is harmful to the ecosystem. Environmental regulations have also become more stringent, causing this waste to become increasingly expensive to dispose. Therefore, exploitation of this waste material as sustainable building material in the construction industry helps preserve the natural resources and also helps maintain the ecological balance. In addition, once the service life of OPS concrete is reached, it may also be possible for reuse as aggregates in the production of recycled aggregate concrete. However, further investigations are required to confirm this on OPS concrete.

OPS is hard in nature and does not deteriorate easily once bound in concrete and therefore, it does not contaminate or leach to produce toxic substances (Basri *et al*. 1999). Unlike artificially produced aggregates or industrial by-products, OPS does not need to be processed or require any chemical pre-treatment before it is used. The bulk density of OPS is about 500 to 600 kg/m^3, producing concretes of about 1900 kg/m^3 in density, which makes them lightweight. It has been found that OPS concrete easily attains the strength of more than 17 MPa (Mannan and Ganapathy 2004), which is a requirement for structural lightweight concrete as per ASTM C330. More recently, compressive strengths of up to 28 MPa have been achieved (Teo *et al*. 2005). The durability of OPS concrete has also been studied previously. When cured in water, it was found that OPS concrete have water absorption and water permeability of about 11% and 6.4 x 10^{-10} cm/s respectively at an age of 28 day (Teo *et al*. 2006), which is comparable to other lightweight concretes such as those made from pumice aggregates (Güdüz and Uğur 2005; Hossain 2004).

Fig. 1 Oil palm shell (OPS) being left at palm oil mill area.

[1]Research Associate, Civil Engineering Program, School of Engineering and Information Technology, Universiti Malaysia Sabah, Malaysia.
[2]Associate Professor, Civil Engineering Program, School of Engineering and Information Technology, Universiti Malaysia Sabah, Malaysia.
E-mail: mannan@ums.edu.my
[3]Associate Professor, Civil Engineering Program, School of Engineering and Information Technology, Universiti Malaysia Sabah, Malaysia.

The use of lightweight concrete in the construction industry has been gaining popularity in the past few decades. Although there have been many works done on the structural performance of lightweight aggregate concrete, these are mostly confined to naturally occurring aggregates, manufactured aggregates and aggregates from industrial by-products. If OPS concrete can be used for structural applications, it would not only be beneficial towards the environment, but also be advantageous for low-income families as this concrete can be used for the construction of low cost houses, especially in the vicinity of oil palm plantations. For structural applications, the flexural behaviour of OPS concrete beams has to be closely scrutinised and clearly established. Therefore, this paper presents the results of an experimental investigation on the flexural behaviour of reinforced OPS concrete beams. The beams were loaded incrementally until failure and their strength, cracking, deformation and ductility behaviour were examined.

2. Comparison between OPS aggregate and conventional granite aggregate

As OPS are organic, the properties of OPS highly differ from the conventional granite aggregates and these are further illustrated in **Table 1**. Due to the porous nature of the OPS aggregate, low bulk density and high water absorption are expected. The low bulk density is advantageous, as the resulting hardened concrete will be much lighter compared to conventional granite concrete. This reduces the overall dead load in a structure, which comes with a significant amount of saving in the total construction cost. In addition, the lightweight nature of the resulting concrete also plays a crucial role in countries where the occurrence of earthquake is inevitable as the catastrophic inertia forces that influence the structures can also be ultimately reduced as these forces are proportional to the weight of the structure.

In general, most lightweight aggregates have higher water absorption values compared to that of conventional aggregate. Although OPS has a high water absorption, even higher water absorptions were recorded for pumice aggregates which have a value of about 37% (Hossain 2004). However, the high water absorption of OPS aggregates can be beneficial to the resulting hardened concrete. It has been reported that lightweight concretes with porous aggregates (high water absorption) are less sensitive to poor curing as compared to normal weight concrete especially in the early ages due to the internal water supply stored by the porous lightweight aggregate (Al-Khaiat and Haque 1998).

It was also observed that the AIV and ACV of OPS aggregate are also much lower compared to granite aggregates. More specifically, the AIV and ACV were approximately 46% and 58% lower respectively compared to the granite aggregates, which shows that OPS is a good shock absorbing material.

3. Experimental program

3.1 Materials and mix proportions

For the purpose of the current investigation, OPS aggregates were used as full replacement for the conventional granite aggregates in the manufacture of lightweight concrete. The materials used in the mix were Ordinary Portland Cement (ASTM Type 1), river sand, OPS and potable water. The properties of OPS used are presented in **Table 1**. In addition, the properties of granite were also provided for comparison purposes. The river sand properties namely the specific gravity, water absorption and fineness modulus were 2.45, 3.89% and 1.40 respectively. A Type-F naphthalene sulphonate formaldehyde condensate based superplasticiser (SP) in aqueous form conforming to ASTM C 494 was incorporated in the mix to increase the workability. All mixes had 510 kg/m^3 cement, 848 kg/m^3 sand, 308 kg/m^3 OPS and 1.4 litres per 100 kg cement with a water/cement ratio of 0.38.

3.2 Reinforced concrete beam details

A total of 6 beams were fabricated and tested. The beams were designed as under-reinforced beams. Three beams were singly reinforced (denoted with ‘S’) and the remaining three were doubly reinforced (denoted with ‘D’). Accompanying the beam test, the required number of cubes, cylinders and prisms were tested on the same day as the beam testing to determine the properties of the concrete and these are presented in **Table 2**. The

Table 1 Properties of aggregates.

Properties	OPS aggregate	Granite aggregate
Maximum aggregate size, mm	12.5	12.5
Shell thickness, mm	0.5 – 3.0	-
Bulk density, kg/m^3	590	1490
Specific gravity (saturated surface dry)	1.17	2.59
Fineness modulus	6.08	6.66
Los Angeles abrasion value, %	4.90	20.30
Aggregate impact value (AIV), %	7.51	13.95
Aggregate crushing value (ACV), %	8.00	19.00
24-hour water absorption, %	33.0	0.67

results are reported as an average of three specimens.

The width (B) and effective depth (d) of the beams were maintained at 150 mm and 200 mm respectively for all beams. The beam sizes and length were chosen to ensure that the beams would fail in flexure (shear span to effective depth ratio = 5.75). The beam dimensions were also sufficiently large to simulate a real structural element. The beam details are shown in **Table 3** and **Fig. 2**. The yield strength, f_y for the tension steel bars were 509, 495, 510 and 528 N/mm^2 for Y10, Y12, Y16 and Y20 respectively. Sufficient shear links were also provided along the beam expect at the pure bending region of 700 mm.

3.3 Beam fabrication, instrumentation and testing

A small part at the midspan of the tension bars (approximately 20 mm in length) was ground smooth to facilitate the fixing of TML strain gauges (model: FLA-10-11) and then protected using silicone gel to avoid accidental damage during pouring of concrete. When more than one layer of steel bars was required, a clear spacing of 20 mm was maintained between the layers. Larger diameter bars were used as the bottom layer when different sizes of bars were involved.

Immediately after casting in wooden formwork, the beams were covered with plastic sheet and left under shed (Temp = 28 ± 5ºC, Relative humidity = 68 – 91%). The sides of the formwork were stripped the following day and moist cured with wet burlap for another 6 days, after which the beams were left in ambient laboratory conditions of 25 ± 3°C and 74 – 88% relative humidity until the age of test. Testing of beams was conducted at an age of about 50 to 60 days.

Before testing commenced, Demec points and TML strain gauges (model: PL-60-11) were attached to the concrete surface in the central region of the beams to measure the strains at different depths as illustrated in Fig. 2. The top surface of the beams was also instrumented with a strain gauge to measure the concrete compressive strains in the pure bending region. LVDTs (linear voltage displacement transducers) were used for measuring deflections at several locations including one at midspan and two directly below the loading points. All strain gauges and LVDTs were connected to a portable data logger from which the readings were captured by a computer at preset load intervals until failure of the beam occurred.

The end rotations of the beams were measured using a theodolite with an accuracy of 1 second. The theodolite was positioned on the beam exactly over the support point (**Fig. 2**) and a measurement staff was placed some distance from the theodolite to observe vertical readings at every load increment.

The test was carried out using a 1,000 kN hydraulic actuator and the beams were subjected to two-point loads under a load control mode with 15 to 25 increments until failure as shown in **Fig. 2**.

The distance between the loading points was kept constant at 700 mm. During testing, the beams were preloaded with a minimal force of 0.5 kN to allow initiation of the LVDTs and strain gauges. The development of cracks was observed and the crack widths were measured using a hand-held microscope with an optical magnification of X40 and a sensitivity of 0.02 mm.

Table 2 Properties of OPS concrete.

Beam type	Singly reinforced	Doubly reinforced
Air-dry density (kg/m^3)	1965	1940
Compressive strength (MPa)	26.3	25.3
Split tensile strength (MPa)	1.82	1.67
Modulus of rupture (MPa)	4.93	4.89
Elastic modulus (GPa)	5.28	5.05

Table 3 Test beam details.

Beam no.	Beam type	Tension reinforcement no. and size	Nominal/ compression reinforcement no. and size	Beam size, B x D (mm)	Area of tensile steel, A_s (mm^2)	$\rho = A_s/bd$, %
S1	Singly	2Y10	2R8	150 x 230	157	0.52
S2	Singly	2Y12		150 x 231	226	0.75
S3	Singly	3Y12		150 x 231	339	1.13
D1	Doubly	3Y16	2Y10	150 x 233	603	2.01
D2	Doubly	3Y20	2Y16 + 1Y12	150 x 235	943	3.14
D3	Doubly	3Y20 + 2Y12	2Y20 + 1Y10	150 x 242	1169	3.90

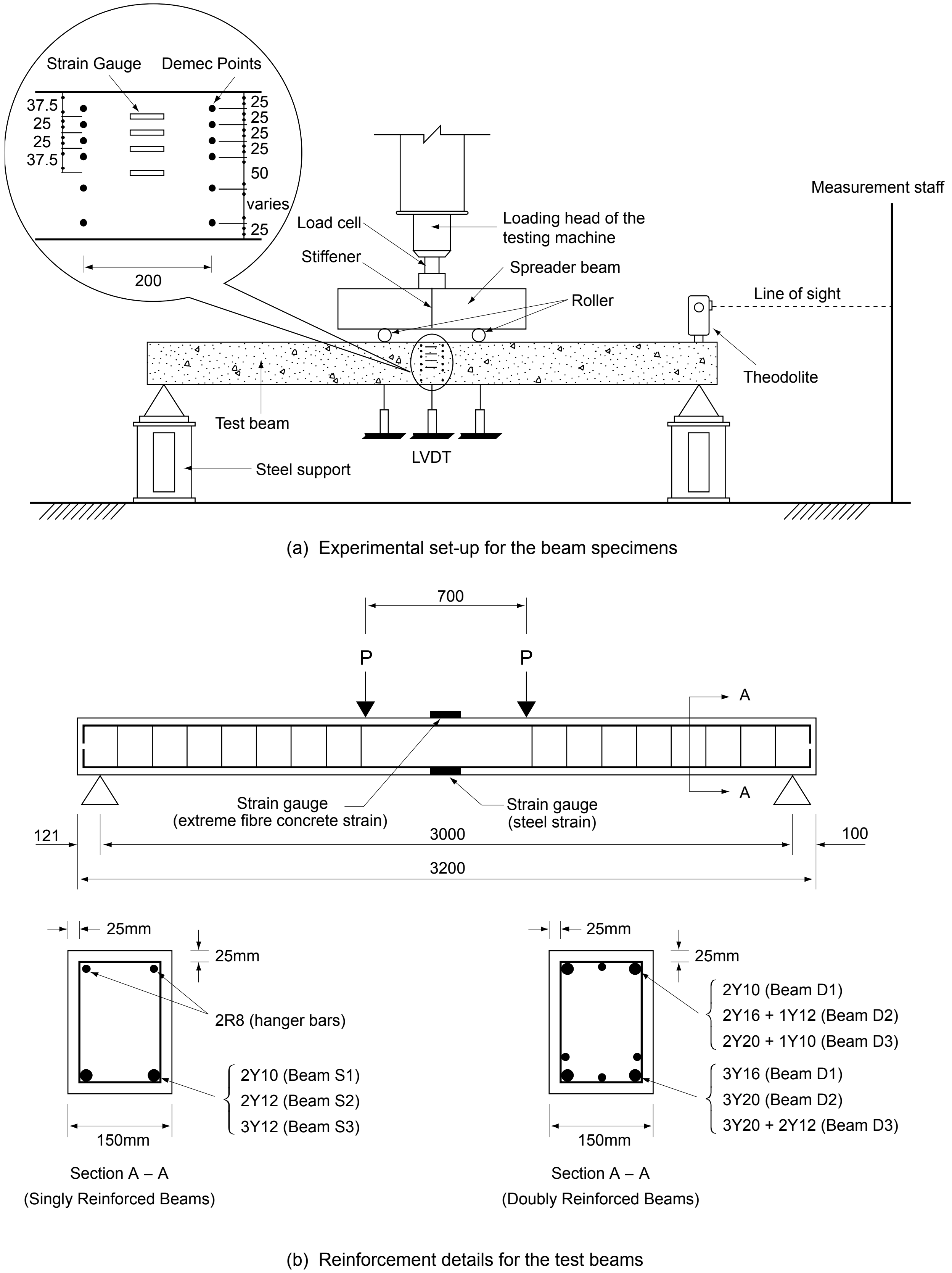

Fig. 2 Testing set-up and beam details.

4. Results and discussions

4.1 General observations

All beams showed typical structural behaviour in flexure. Since the concave and convex surfaces of the OPS aggregates are fairly smooth, bond failure may occur during testing. However, no horizontal cracks were observed at the level of the reinforcement, which indicated that there were no occurrences of bond failure. Vertical flexural cracks were observed in the constant-moment region and final failure occurred due to crushing of the compression concrete with significant amount of ultimate deflection. Since all beams were under-reinforced, yielding of the tensile reinforcement occurred before crushing of the concrete cover in the pure bending zone. When maximum load was reached, the concrete cover on the compression zone started to spall. Eventually, crushing of the concrete cover occurred during failure. At failure, the crushing depth of the concrete varied from 60 to 120 mm.

4.2 Bending moments

A comparison between the experimental ultimate moments (M_{ult}) and the theoretical design moments are shown in **Table 4**. The theoretical design moment (M_{des}) of the beams was predicted using the rectangular stress block analysis as recommended by BS 8110. For beams with reinforcement ratios of 3.14% or less, the ultimate moment obtained from the experiment was approximately 4% to 35% higher compared to the predicted values. However, for high reinforcement ratios, i.e. at 3.9%, the experimental ultimate moment was about 6% lower. From the performed tests, it was observed that for OPS concrete beams, BS 8110 can be used to obtain a conservative estimate of the ultimate moment capacity and also provide adequate load factor against failure for reinforcement ratios up to 3.14%.

4.3 Deflection behaviour

Figures 3 and **4** show the typical experimental moment-deflection curves for the singly and doubly reinforced beams respectively. In all beams, before cracking occurred, the slope of the moment-deflection curve was steep and closely linear. Once flexural cracks formed, a change in slope of the moment-deflection curve was observed and this slope remained fairly linear until yielding of the steel reinforcement took place. From the deflection curves, it can be observed that OPS concrete beams exhibit behaviour similar to that of other lightweight concrete beams (Swamy and Ibrahim 1975; Swamy and Lambert 1984).

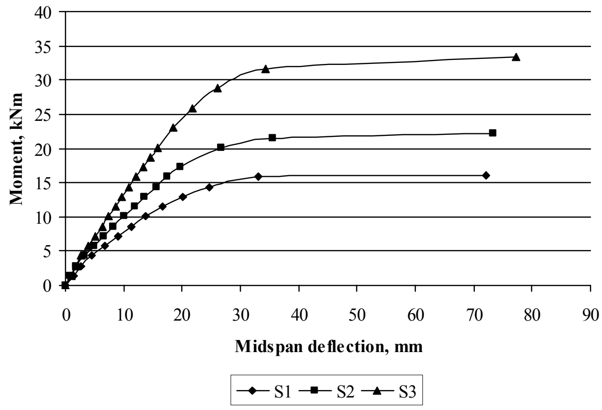

Fig. 3 Experimental moment-deflection curve for singly reinforced beams.

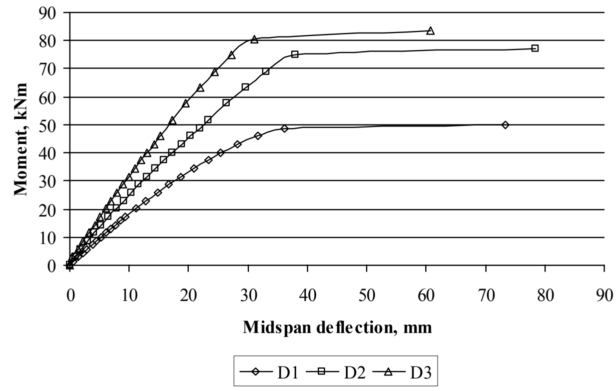

Fig. 4 Experimental moment-deflection curve for doubly reinforced beams.

Table 5 compares the predicted midspan deflection under service moments with the experimental values. The predicted deflection is calculated from the beam curvatures according to BS 8110, using the formula

Table 4 Comparison between experimental and theoretical ultimate moments.

Beam no.	(1) Neutral axis depth at ultimate moment (mm)	(2) Experimental ultimate moment, M_{ult} (kNm)	(3) Theoretical design moment, M_{des}, (kNm)	(4) Capacity ratio of OPS concrete beams (2)/(3)
S1	50.03	16.10	13.60	1.23
S2	67.20	22.14	18.07	1.17
S3	81.12	33.35	24.73	1.35
D1	137.01	50.03	42.46	1.18
D2	140.18	77.05	73.87	1.04
D3	155.30	83.38	89.09	0.94

$$\Delta = K\ell^2\kappa \quad (1)$$

where Δ = midspan deflection, K = a constant depending upon the distribution of bending moments of a member, ℓ = effective span and κ = curvature of beam. It was observed that the deflection obtained from the experiment at the service moments compares reasonably well to the predicted deflection recommended by BS 8110. The service moment was obtained based on the load factor method of BS8110 for reinforced concrete beams.

The modulus of elasticity of concrete is very much governed by the stiffness of the coarse aggregates. From the properties in **Table 1**, it can be seen that OPS is porous in nature and it also has low density, which directly influences the stiffness of the aggregate. This results in a concrete with low modulus of elasticity. Although OPS concrete has low modulus of elasticity, the deflection under the design service loads for the singly reinforced beams is acceptable as the span-deflection ratios ranged between 252 to 263 and are within the allowable limit provided by BS 8110. BS 8110 recommends an upper limit of span/250 for the deflection in order to satisfy the appearance and safety criteria of a structure. For the doubly reinforced beams, the span-deflection ratio ranged from 146 to 196. Hence, for higher reinforcement ratios (higher load carrying capacity), it is recommended that larger beam depths should be employed. However, it must be noted that, in order to obtain a complete understanding on the deflection behaviour, further investigations incorporating the effects of creep and shrinkage on the concrete are required.

4.4 Ductility behaviour

The ductility of reinforced concrete structures is also of paramount importance because any member should be capable of undergoing large deflections at near maximum load carrying capacity, providing ample warning to the imminence of failure. In this study, the displacement ductility was investigated. **Table 6** shows the ductility of the tested OPS concrete beams. The displacement ductility ratio is taken in terms of $\mu = \Delta_u / \Delta_y$, which is the ratio of ultimate to first yield deflection, where Δ_u is the deflection at ultimate moment and Δ_y is the deflection when steel yields. In general, high ductility ratios indicate that a structural member is capable of undergoing large deflections prior to failure. In this investigation, it was observed that for beams with reinforcement ratios up to 2.01%, the ductility ratio was more than 3, which shows relatively good ductility. One of the factors contributing to the good ductility behaviour of the OPS beams was the toughness and good shock absorbance nature of the OPS aggregates as indicated by the aggregate crushing value (ACV) and aggregate impact value (AIV) from **Table 1**. Ashour (2000) mentions that members with a displacement ductility in the range of 3 to 5 has adequate ductility and can be considered for structural members subjected to large displacements, such as sudden forces caused by earthquake. From this investigation, it was also observed that a higher tension reinforcement ratio results in less ductile behavior. This is in agreement with the work of other researchers (Lee and Pan 2003; Rashid and Mansur 2005).

Table 5 Deflection of OPS concrete beams at service moment.

Beam no.	Theoretical design service moment, Ms (kNm)	Deflection from experiment, Δ_{exp} (mm)	Theoretical deflection, $\Delta_{theo,}$ BS 8110 (mm)	$\Delta_{exp}/\Delta_{theo}$	Span/$\Delta_{exp.}$
S1	8.654	11.40	10.75	1.06	263
S2	11.454	11.70	12.76	0.92	256
S3	15.611	11.90	13.90	0.86	252
D1	26.709	15.30	15.90	0.96	196
D2	46.322	20.50	18.35	1.12	146
D3	55.614	18.80	15.50	1.21	159

Table 6 Displacement ductility of OPS concrete beams obtained from experiment.

Beam no.	Yield stage		Ultimate Stage		Displacement ductility ratio, Δ_u / Δ_y
	Moment, kNm	Deflection, Δ_y (mm)	Moment, kNm	Deflection, Δ_u (mm)	
S1	11.500	16.64	16.100	72.18	4.34
S2	15.813	17.48	22.138	73.40	4.20
S3	25.875	21.72	33.350	77.20	3.55
D1	37.375	23.34	50.025	73.26	3.14
D2	63.250	29.56	77.050	78.38	2.65
D3	69.000	24.40	83.375	60.76	2.49

4.5 Cracking behaviour

Crack widths were measured at every load interval at the tension steel level and the crack formations were marked on the beam. For the doubly reinforced beams, initial cracking occurred at about 5 to 9% of the ultimate load, whereas for the singly reinforced sections, the cracks formed at about 11 to 15% of the ultimate load. This reveals that for higher reinforcement ratios, the first crack occurs at a smaller percentage of the ultimate load. It was noticed that the first crack always appears close to the midspan of the beam. The cracks forming on the surface of the beams were mostly vertical, suggesting failure in flexure. The cracking characteristics of OPS concrete beams are illustrated in **Table 7**.

The theoretical cracking moment, $M_{CR(theo)}$ of the beam is determined using the formula as recommended by ACI 318,

$$M_{CR(theo)} = \frac{f_r \times I_g}{y_t} \quad (2)$$

where f_r = modulus of rupture of concrete (MPa); I_g = second moment of inertia of gross area ignoring reinforcement and y_t = distance from the extreme tension fibre to the neutral axis. It was observed that the experimental cracking moments were about 35% to 80% of the theoretical cracking moments. The first crack moment is taken as the point where a sudden deviation from the initial slope of the moment-deflection curve occurs. The use of the modulus of rupture greatly overestimates the experimental cracking moments. It is therefore recommended that a reduced value of about 55% of f_r should be used to predict the cracking moment with better accuracy.

Table 8 also compares the predicted crack width according to ACI 318 and BS 8110 under service loads with the experimental values. It was observed that both ACI 318 and BS 8110 code gave reasonably close predictions of the crack width. However, ACI 318 predicts the experimental crack widths of OPS beams with better accuracy compared to BS 8110.

In most codes of practice, the maximum allowable crack widths lie in the range of 0.10 to about 0.40 mm, depending upon the exposure condition. For members protected against weather, ACI 318 permits crack widths up to 0.41 mm. It was observed that for OPS concrete, the crack widths at service load were below the maximum allowable value as stipulated by BS 8110 for durability requirements.

The average crack spacings for the OPS beams were between 77 mm to 107 mm and this is comparable the lightweight aggregate concrete made of expanded slate (Solite) and expanded shale (Aglite) (Swamy and Ibrahim 1975).

4.6 End rotation

The moment-end rotation curves of OPS concrete beams are presented in **Figs. 5** and **6**. The end rotations reflect on the curvature of a beam. From the figure, it can be seen that the shape of the moment-end rotation

Table 7 Cracking characteristics of OPS concrete beams.

Beam no.	Experimental cracking moment, $M_{CR(exp)}$ (kNm)	Theoretical cracking moment, $M_{CR(theo)}$ (kNm)	Theoretical design service moment, M_S (kNm)	Experimental crack width at M_S (mm)	Experimental crack width at failure (mm)	Average crack spacing, (mm)	No. of cracks between loading points
S1	2.300	6.520	8.650	0.22	1.24	107	6
S2	2.875	6.577	10.385	0.22	0.90	77	8
S3	3.738	6.577	16.190	0.22	0.82	90	8
D1	4.313	6.637	26.710	0.26	1.10	99	8
D2	4.313	6.751	45.132	0.26	1.00	92	7
D3	5.750	7.159	55.850	0.27	0.80	80	10

Table 8 Comparison between predicted and experimental crack widths at service loads.

(1) Beam no.	(2) Experimental crack width (mm)	(3) Theoretical crack widths, BS 8110 (mm)	(4) Theoretical crack widths, ACI (mm)	(2)/(3)	(2)/(4)
S1	0.22	0.19	0.23	1.16	0.96
S2	0.22	0.19	0.22	1.16	1.00
S3	0.22	0.19	0.22	1.16	1.00
D1	0.26	0.23	0.19	1.13	1.37
D2	0.26	0.30	0.23	0.87	1.13
D3	0.27	0.37	0.23	0.73	1.17

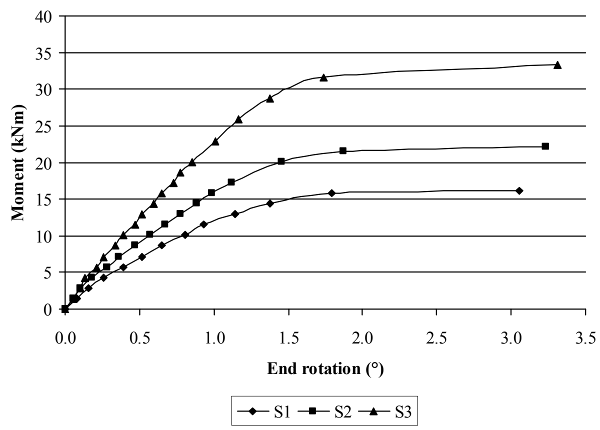

Fig. 5 Experimental end rotations for singly reinforced beams.

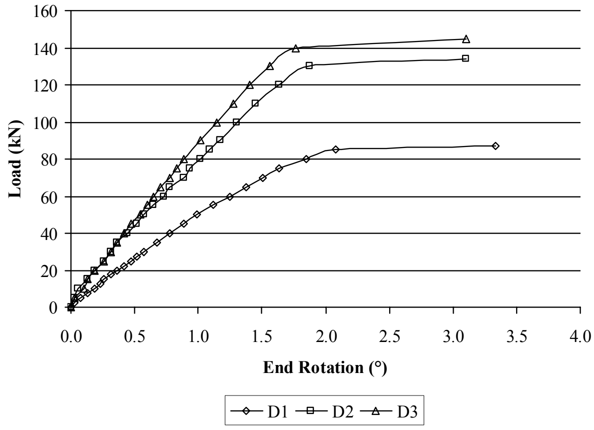

Fig. 6 Experimental end rotations for doubly reinforced beams.

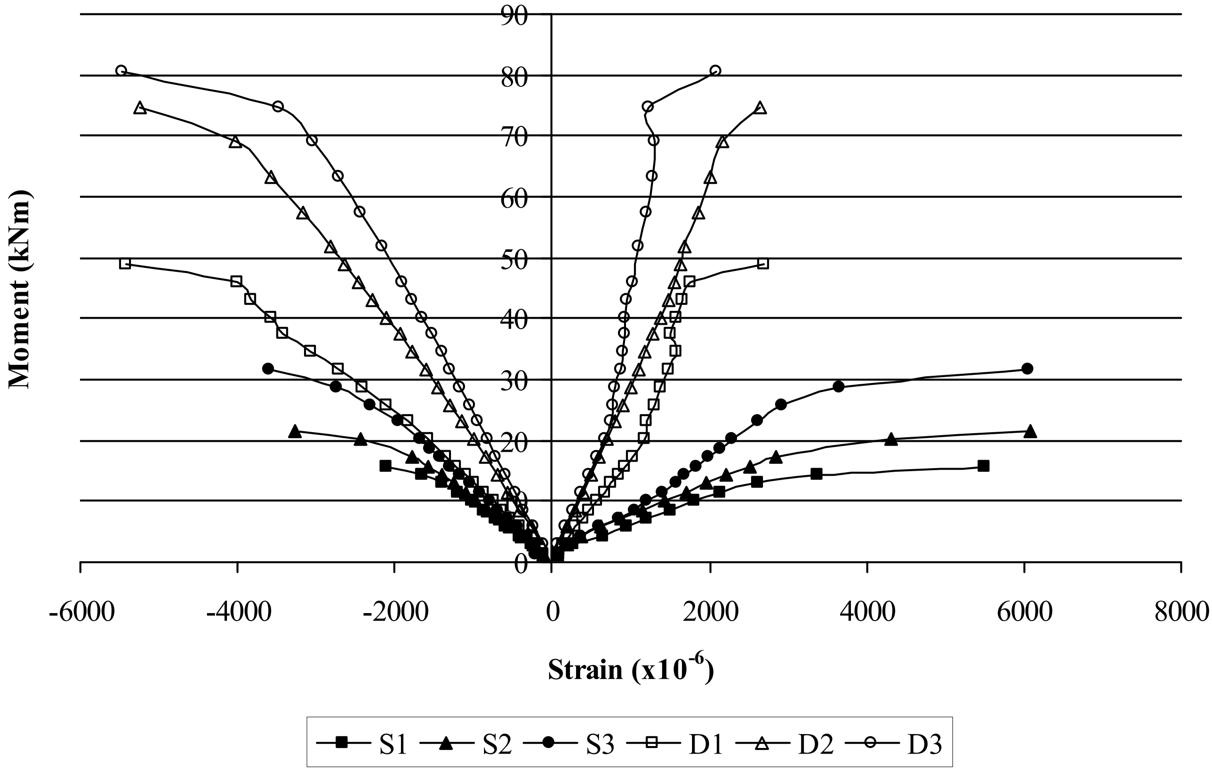

Fig. 7 Strain distributions during loading.

curve follows the general behaviour of a moment-curvature curve, in which it increases linearly until yielding of steel occurred. Once yielding occurred, there was a rapid increase in the end rotations with very little increase in the moment. It was observed that the end rotation of the beams just prior to failure varied from 3° 3' 9.79" to 3° 20' 19.83" and this is comparable to other lightweight concretes (Swamy and Lambert 1984).

4.7 Concrete and steel strains

The concrete and steel strains were measured at every load increments. The strain distribution for the concrete and steel are presented in **Fig. 7**. At service loads, the concrete compressive strains ranged from 498 to 1303 x 10^{-6}. The measured concrete strains and steel strains just prior to failure varied from 2105 to 5480 x 10^{-6} and 2093 to 6069 x 10^{-6} respectively. It must be noted however, that the strain readings were taken at approximately 95% of the failure load and therefore, the actual strain values are much higher than reported herein. Nevertheless, the values obtained are consistent with the works of other researchers (Swamy and Ibrahim 1975;

Swamy and Lambert 1984). These results also show that OPS concrete is able to achieve its full strain capacity under flexural loadings.

5. Conclusions

From the experimental investigation, it was generally observed that the flexural behaviour of OPS concrete is comparable to that of other types of lightweight concretes and this investigation gives encouraging results for OPS to be used as coarse aggregate in the production of structural lightweight concrete especially for the construction of low cost houses. The following observations and conclusions can be made on the basis of the current experimental results.

(1) All OPS concrete beams showed typical structural behaviour in flexure. Since the beams were under-reinforced, yielding of the tensile reinforcement occurred before crushing of the compression concrete in the pure bending zone.

(2) The ultimate moments predicted using BS 8110 provides a conservative estimate for OPS concrete beams up to a reinforcement ratio of 3.14%, with experimental ultimate moments of approximately 4% to 35% higher compared to the predicted moments. For the beam with 3.90% reinforcement ratio, BS 8110 underestimates the ultimate moment capacity by about 6%.

(3) The deflections of OPS concrete calculated using BS 8110 under service loads can be used to give reasonable predictions. The deflection under the design service loads for the singly reinforced beams were within the allowable limit provided by BS 8110. For the doubly reinforced beams, the deflections at service loads exceeded the limit, suggesting that the beam depths should be increased.

(4) OPS concrete beams showed good ductility behaviour. All beams exhibited considerable amount of deflection, which provided ample warning to the imminence of failure.

(5) The crack widths at service loads ranged between 0.22 mm to 0.27 mm and this was within the maximum allowable value as stipulated by BS 8110 for durability requirements.

Acknowledgement

This project is funded by Ministry of Science, Technology and Innovation, Malaysia under IRPA research grant no. 03-02-10-0033-EA0031.

References

ACI 318, (1995). "*Building code requirements for reinforced concrete*." Detroit: American Concrete Institute.

Al-Khaiat, H. and Haque, M. N. (1998). "Effect of initial curing in early strength and physical properties of a lightweight concrete." *Cement and Concrete Research*, 28(6), 859-866.

Ashour, S. A. (2000). "Effect of compressive strength and tensile reinforcement ratio on flexural behaviour of high-strength concrete beams." *Engineering Structures*, 22(5), 413-423.

ASTM C 330. *Standard specification for lightweight aggregates for structural concrete*. Annual Book of ASTM Standards.

ASTM C 494. *Standard Specification for Chemical Admixtures for Concrete*. Annual Book of ASTM Standards.

Basri, H. B., Mannan, M. A. and Zain, M. F. M. (1999). "Concrete using waste oil palm shells as aggregate." *Cement and Concrete Research*, 29(4), 619-622.

BS 8110, (1985). "*Structural use of Concrete Part 1.Code of Practice for Design and Construction.*", London: British Standard Institution.

Güdüz, L. and Uğur, İ. (2005). "The effects of different fine and coarse pumice aggregate/cement ratios on the structural concrete properties without using any admixtures." *Cement and Concrete Research*, 35(9), 1859-1864.

Hossain, K. M. A. (2004). "Properties of volcanic pumice based cement and lightweight concrete." *Cement and Concrete Research*, 34(2), 283-291.

Lee, T. K. and Pan, A. D. E. (2003). "Estimating the relationship between tension reinforcement and ductility of reinforced concrete beam sections." *Engineering Structures*, 25(8), 1057-1067.

Ma, A. N., Toh, T. S. and Chua, N. S. (1999). "Renewable energy from oil palm industry." *In: Singh G., Lim K. H., Teo L. and Lee D. K., Oil palm and the Environment: A Malaysian Perspective*, Malaysian Oil Palm Growers' Council, Kuala Lumpur, Malaysia, 253-259.

Malaysian Palm Oil Board (MPOB) 2006. "A summary on the performance of the Malaysian oil palm industry – 2005 [on-line]." Available from: <http://econ.mpob.gov.my/economy/summary_latest05.htm> [Assessed on 5 July 2006].

Mannan, M. A. and Ganapathy, C. (2004). "Concrete from an agricultural waste-oil palm shell (OPS)." *Building and Environment*, 39(4), 441-448.

Rashid, M. A. and Mansur, M. A. (2005). "Reinforced high-strength concrete beams in flexure." *ACI Structural Journal*, 102(3), 462-471.

Swamy, R. N. and Ibrahim, A. B. (1975). "Flexural behaviour of reinforced and prestressed Solite structural lightweight concrete beams." *Building Science*, 10(1), 43-56.

Swamy, R. N. and Lambert, G. H. (1984). "Flexural behaviour of reinforced concrete beams made with fly ash coarse aggregates." *The International Journal of Cement Composites and Lightweight Concrete*, 6(3), 189-200.

Teo, D. C. L., Mannan, M. A., Kurian, V. J. and Ganapathy, C. (2006). "Lightweight concrete made from oil palm shell (OPS): Structural bond and durability properties." *Building and Environment*, In Press, DOI: 10.1016/j.buildenv.2006.06.013.

Teo, D. C. L., Mannan, M. A. and Kurian, V. J. (2005). "Structural performance of lightweight concrete." *In: Conference on Sustainable Building Southeast Asia*, Kuala Lumpur 11-13 April 2005, 254-258.